Physical Processes in Supernova Remnants

Evolution of Massive Stars

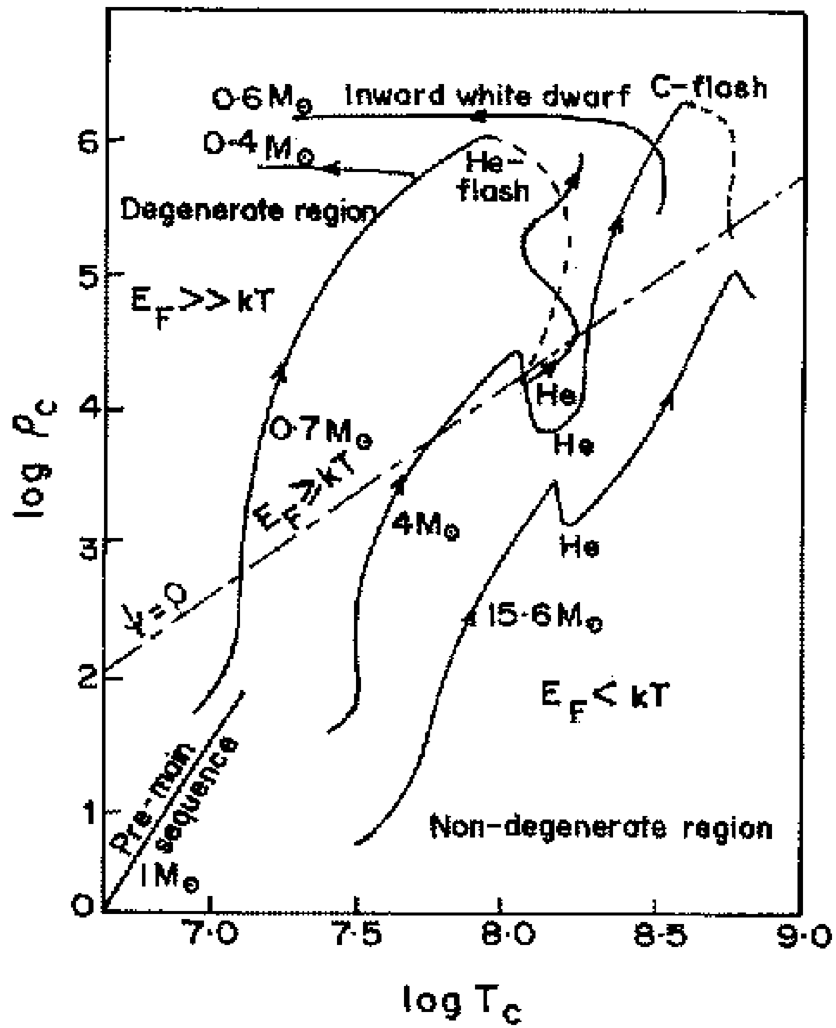

Stars with masses less than 9 $M_\odot$ do not burn carbon – Stars with masses near 9 $M_\odot$ develop a degenerate carbon core and have a "C-flash", due to C-burning in a non-degenerate shell.

Stars having masses higher than 9 $M_\odot$ do not develop degenerate cores, burn carbon up to the formation of an iron core.

If $T_c > 5 \times 10^9$ K , statistical equilibrium is destroyed and photo-disintegration of iron dominates.

$$\gamma + Fe^{56} \rightarrow 13He^4 + 4n - 2.2MeV / nuc$$

This process absorbs to much thermal energy, destroying hydrostatic equilibrium and producing the gravitational collapse of the star.

The explosion mechanism

The photo-disintegration of iron destabilizes the star – the core collapses first since $t_{col} \propto (G\rho)^{-1/2}$ and the beta capture process forms a neutron rich core having a mass close to the Chandrasekhar limit (1.4 $M_\odot$).

$$X(A,Z)+e^- \rightarrow X(A,Z-1)+\nu_e$$

The energy released under the form of neutrinos (URCA and thermal), having an average energy of 2 MeV, is of the order of the potential energy of the neutron core with a radius of about 100 km

$$\frac{GM_c^2}{R_c} \simeq 5\times10^{52} erg \quad \Rightarrow \quad N_\nu \approx 2\times10^{58}$$

Once the core is formed (timescale around few ms) the outer envelope falls into the core and bounces, absorbing the neutrinos that transfer momentum to the matter, producing ejection.

If the transfer conditions are not adequate, there is no ejection and the envelope falls back, being accreted by the core, which collapses to form a black hole (case of stars with masses higher than ~ 50 $M_\odot$)

The explosion mechanism

The momentum carried by each neutrino is E_ν / c and the efficiency of each transfer is *f* . Since each neutrino suffers on the average N_s elastic scatterings inside the envelope, the total momentum transferred is

$$\Delta P_\nu \simeq f\left(\frac{E_\nu}{c}\right) N_\nu N_s \simeq 2.3\times 10^{45} f \quad g.cm.s^{-1}$$

Since the total number of scatterings is of the order of the square of the neutrino optical depth

$$N_s \simeq \tau_\nu^2 = \left(\frac{\sigma_\nu}{m_n}\Sigma\right)^2 \approx 1100 \quad with\ \sigma_\nu \approx 9.5\times 10^{-45}\left(\frac{E_\nu}{MeV}\right)\ cm^2 \quad and \quad \Sigma \approx 10^{23}\ \ g/cm^2$$

Observed momentum $\longrightarrow$ $M_{ejec} V_{eje} = 6.0\times 10^{42}\left(\frac{M_{ejec}}{10 M_\odot}\right)\left(\frac{V_{eje}}{3000 km/s}\right)$

Required neutrino transfer efficiency $\longrightarrow$ $f \cong 2 \times 10^{-3}$

The Ejected Shell

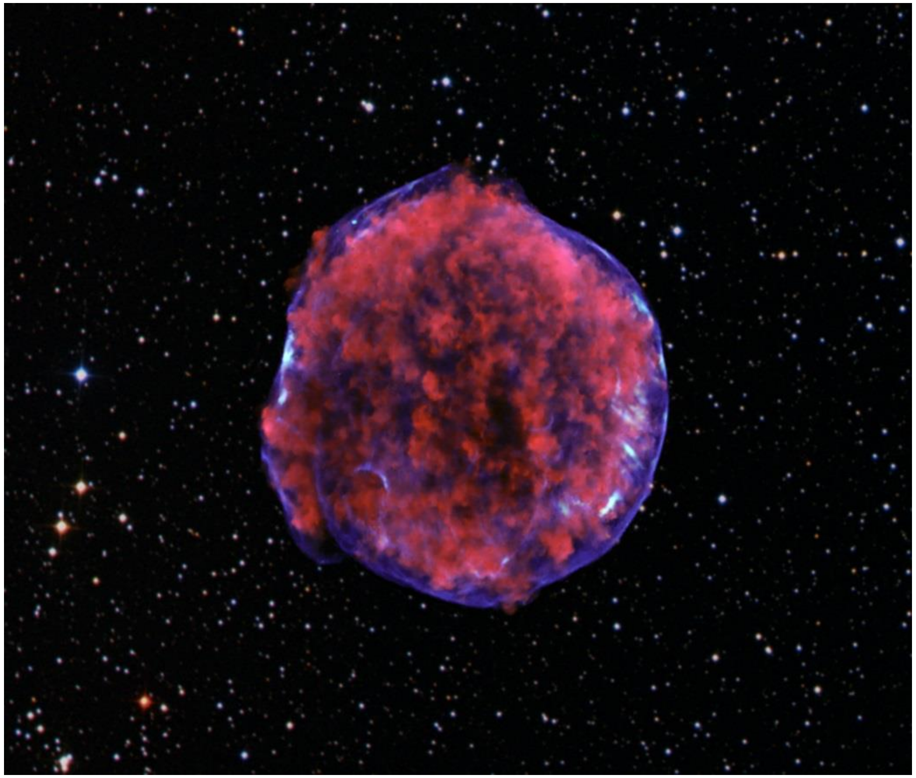

Tycho–Brahe SNR – image composite: radio, optical and X-rays obtained by the satellite Chandra

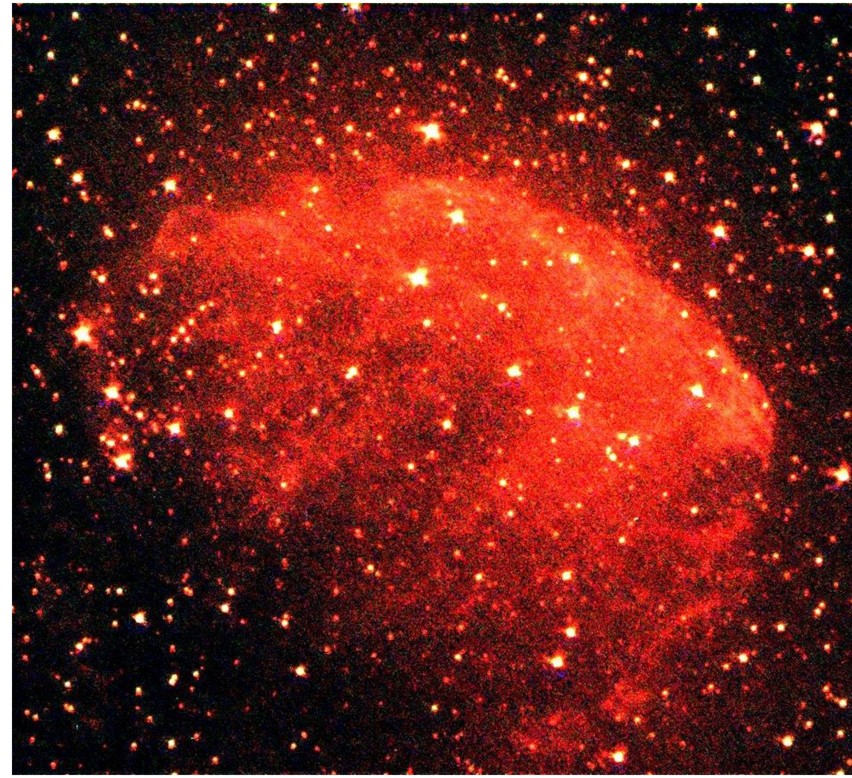

IC 433 – SRN – image taken with an H-alpha filter using a 15cm refractor and a modified Canon 1200D camera. Non-thermal X-rays are emitted from this SNR

Sketch of the structure of the SNR shell

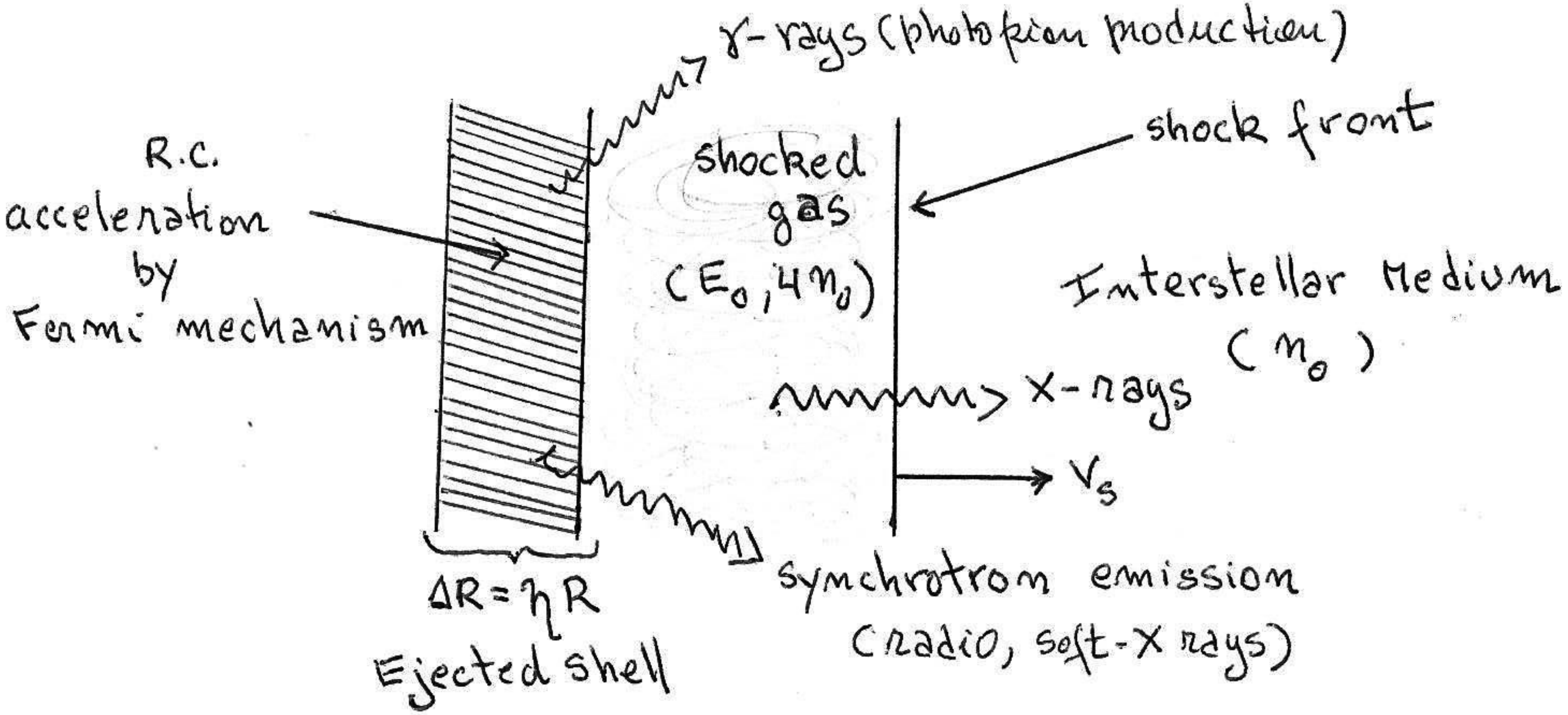

Phases of Expansion

- **Phase I** – "free-expansion" – short phase in which the shell velocity is constant – valid when the ejected mass is less than the mass swept by expansion through the interstellar gas.

- **Phase II** – adiabatic or Sedov phase – the cooling timescale is longer than the expansion timescale.

- **Phase III** – the expansion timescale becomes longer than the cooling – the shell expands according to the momentum conservation law.

The motion of the shock front – Phase II (Sedov)

Using the Hugoniot-Rankine equations: $$\begin{cases} P_s = 2\dfrac{\rho_I V_s^2}{(\gamma+1)} + \dfrac{(\gamma-1)}{(\gamma+1)} P_I \\ \dfrac{\rho_I}{\rho_s} = \dfrac{(\gamma-1)}{(\gamma+1)} + \dfrac{2\gamma}{(\gamma+1)} \dfrac{P_I}{(\rho_I V_s^2)} \end{cases}$$

For a strong shock $\longrightarrow$ $$P_s \gg P_I \quad and \quad P_I \ll \rho_I V_s^2$$

Consequently $\longrightarrow$ $$\frac{\rho_I}{\rho_s} \approx \frac{1}{4} \quad and \quad P_s \approx \frac{3}{4}\rho_I V_s^2 \Rightarrow also\ \frac{P_s}{\rho_s} = \frac{kT_s}{\mu m_p} \approx \frac{3}{16} V_s^2$$

But $\longrightarrow$ $$P_s = \frac{2}{3}\frac{E_{th}}{(4\pi R_s^3/3)} = \frac{E_{th}}{2\pi R_s^3} \Rightarrow V_s = \frac{dR_s}{dt} = \left(\frac{2E_{th}}{3\pi\rho_I}\right)^{1/2} R_s^{-3/2}$$

Integrating $\longrightarrow$ $$R_s = At^{2/5} \quad with \quad A = \left(\frac{25}{6\pi}\frac{E_{th}}{\rho_I}\right)^{1/5} \quad and \quad V_s = \frac{2}{5}\frac{R_s}{t}$$

Shock motion in Phase III

Gas has cooled – the thermal pressure is no longer important – eq. motion is simply

$$\frac{d}{dt}\left(M_s V_s\right) = 0 \;\Rightarrow\; \frac{4\pi}{3}\rho_I R_s^3 \frac{dR_s}{dt} = K$$

Integrating $\longrightarrow$ $R_s \approx B t^{1/4} \quad with \quad B = \left(\frac{3K}{\pi\rho_I}\right)^{1/4} \quad and \quad V_s = \frac{1}{4}\frac{R_s}{t}$

The constant *K* can be estimated by assuming that the transition from phase II to phase III occurs at the cooling timescale

Then $\longrightarrow$ $A t_c^{2/5} \approx B t_c^{1/4} \quad \Rightarrow \quad K = \frac{\pi}{3}\rho_I^{1/5}\left(\frac{25 E_{th}}{4\pi}\right)^{4/5} t_c^{3/5}$

Where $\longrightarrow$ $t_c = E_{th} / L_B$ and L_B is the radiation rate of the shell due to line and

bremsstrahlung emission

Some difficulties with phase II

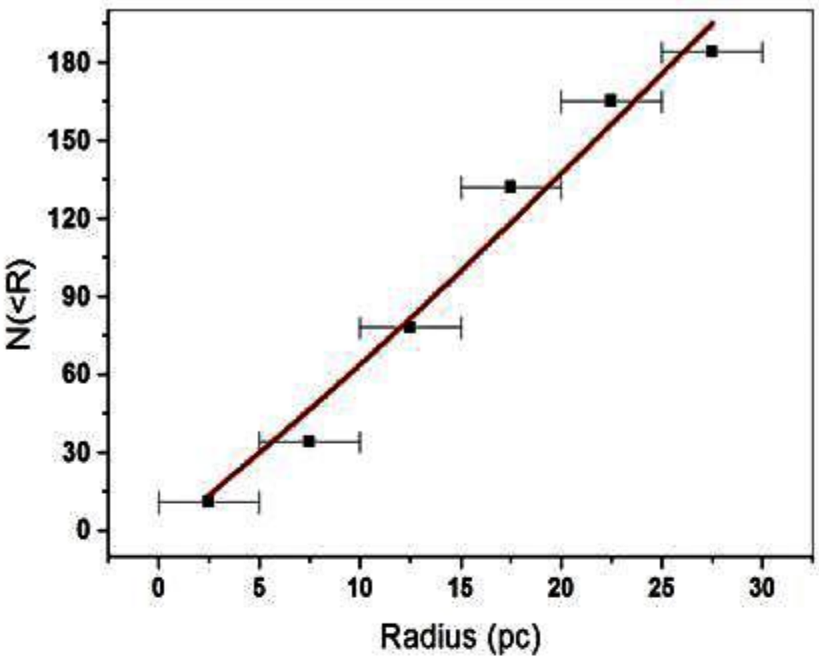

Let ν_{II} the rate at which type II supernovae are formed in the Galaxy. Then the number of SNR with radius less or equal R_S is given by

$$\frac{dN_{SN}}{dt} = \frac{dN_{SN}}{dR_s}\frac{dR_s}{dt} = \nu_{II}$$

Using the previous results for V_S and integrating

$$N(<R_s) = \frac{3}{5}\frac{\nu_{II}}{A^{5/2}}R_s^{5/2}$$

Plot of the quantity $N(<R_S)$ vs the shell radius using data from the Green catalog. The best data fit gives

$$N(<R_s) = (4.92 \pm 1.99) R_s^{(1.11 \pm 0.13)}$$

A similar result was obtained for SNR in the Large Magellanic Cloud, excluding uncertainties in the distance scale as a possible explanation for such a discrepancy.

Synchrotron Emission from the Shell

Shell luminosity $\longrightarrow$ $4\pi D^2 f_\nu = L_\nu = B_\gamma K_e H^{(\gamma+1)/2}(4\pi\eta R_s^3)\nu^{-\alpha}$

where the shell thickness = $\Delta R_s = \eta R_s$ and $\alpha = (\gamma-1)/2$

Emission coefficient: $$B_\gamma = \frac{3}{16\pi}\left(\sqrt{\frac{27}{32\pi^2}}\right)^{(\gamma-3)/2} \sigma_T c^{(\gamma-1)/2}(mc^2)^{(5-3\gamma)/2} e^{(\gamma-3)/2}$$

Relativistic electron density: $$W_e = \int_0^\infty EN(E)dE = \int_0^\infty E\frac{K_e}{(E+mc^2)^\gamma}dE = \frac{K_e}{(\gamma-2)(\gamma-1)(mc^2)^{\gamma-2}}$$

Total cosmic ray energy density: $W_{CR} = W_p + W_e = \beta W_e$ with $\beta = \left(\frac{m_p}{m}\right)^{(\gamma-1)/2}$

From these eqs.: $\beta L_\nu = B_\gamma(\gamma-2)(\gamma-1)(mc^2)^{\gamma-2} W_{CR} H^{(\gamma+1)/2}\Omega_{sh}\nu^{-\alpha}$

Using the previous eqs., the energy under the form of cosmic rays is:

$$E_{CR} = W_{CR}\Omega_{sh} = \frac{\beta L_\nu}{(\gamma-2)(\gamma-1)B_\gamma (mc^2)^{\gamma-2} H^{(\gamma+1)/2}} = \frac{C_{CR}}{H^{(\gamma+1)/2}}$$

The total energy inside the shell $\longrightarrow$ cosmic rays + magnetic field

$$E_T = \frac{C_{CR}}{H^{(\gamma+1)/2}} + \frac{H^2}{8\pi}\Omega_{sh}$$ - Assume that the value of the H-field minimizes the energy

$$\frac{\partial E_T}{\partial H} = 0 \quad \Rightarrow \quad H_{\min} = \left[\frac{2\pi(\gamma+1)C_{CR}}{\Omega_{sh}}\right]^{2/(\gamma+5)} \qquad \Rightarrow \quad E_{CR} = \frac{4}{(\gamma+1)} E_{mag}$$

Catalogs of SNR provide besides position, the energy flux at frequency ν, the spectral index α and the angular diameter θ_s. Since $\gamma = 2\alpha+1$, from observations, the magnetic field (minimum) can be derived if the distance *D* is known

$$H_{\min} = \left[\frac{16\pi(\gamma+1)\beta}{(\gamma-2)(\gamma-1)B_\gamma (mc^2)^{\gamma-2}}\right]^{2/(\gamma+5)} \left(\frac{\nu^\alpha f_\nu}{\eta\theta_s^3 D}\right)^{2/(\gamma+5)}$$

Then, previous eqs. give the cosmic ray energy inside the shell

Example – The Crab Nebula

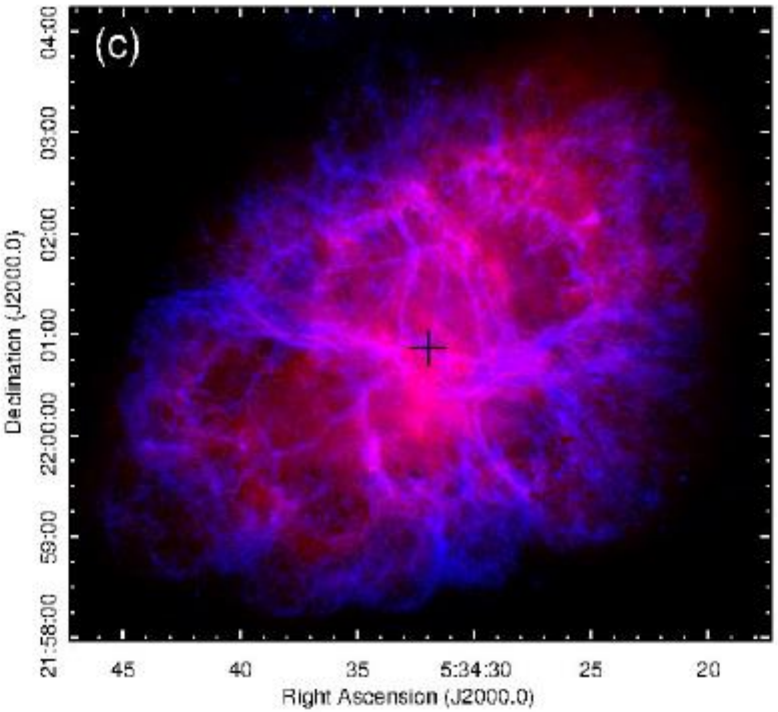

Composite image: red color – radio emission at 3 GHz – blue color – optical emission ([OIII] line) from filaments (image ESA)

Mass under the form of filaments – 2 M⊙; mass of the pulsar – 1.4 M⊙; possible losses from the wind of the progenitor – 3 to 4 M⊙; estimated progenitor mass around 6.4 – 7.4 M⊙, less than the minimal mass for C-burning

Estimated distance 1.9 kpc; average shell radius R_s = 1.53 pc; spectral index α = 0.55; CR power spectrum - $\gamma = 2\alpha+1 = 2.1$

Mean magnetic field – H = 157 mG and mean magnetic+CR energy density = 2.2×10^{-7} erg/cm^3

Observed acceleration of filaments:

$$<\ddot{R}_s> = 7.3\times10^{-4}\, cm/s^2$$

$$<M><\ddot{R}_s> = \frac{4\pi}{3}(\omega_H + \omega_{CR})R_s^2 \quad \Rightarrow \; <M> = 14M_\odot$$

Distance Scale for SNR

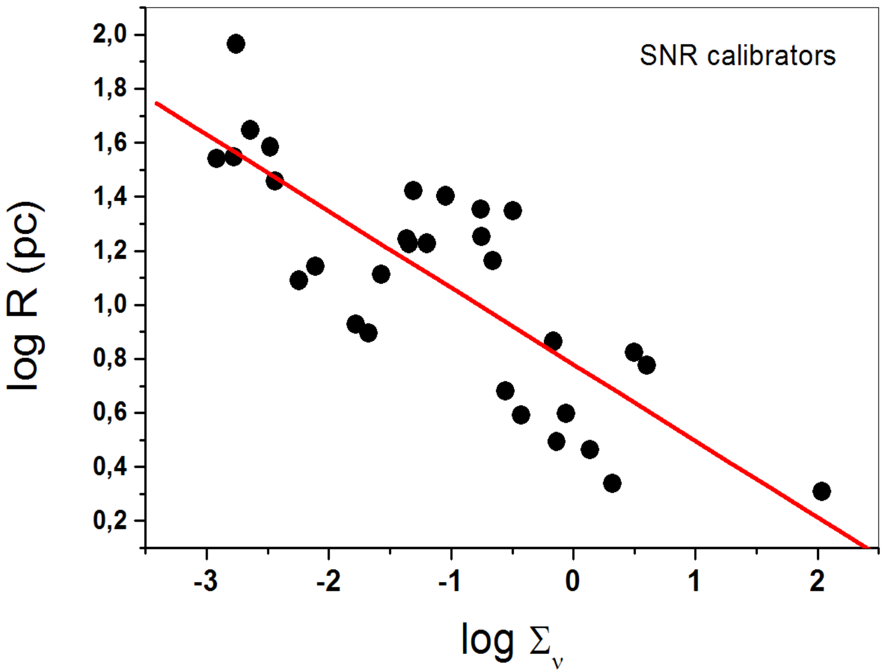

Distances must be calibrated using observable parameters

Define the reduced brightness

$$\Sigma_\nu = f_\nu / \theta_s^2$$

There is a relation between the radius of the shell and the reduced brightness.

Calibration of the Σ x R relation using 30 SNR with distances derived with errors not larger than 50%

$$\log R = 0.780 - 0.283 \log \Sigma_\nu \pm 0.255 \qquad c.r. = 0.805$$

Shell parameters: H-field & CR energy

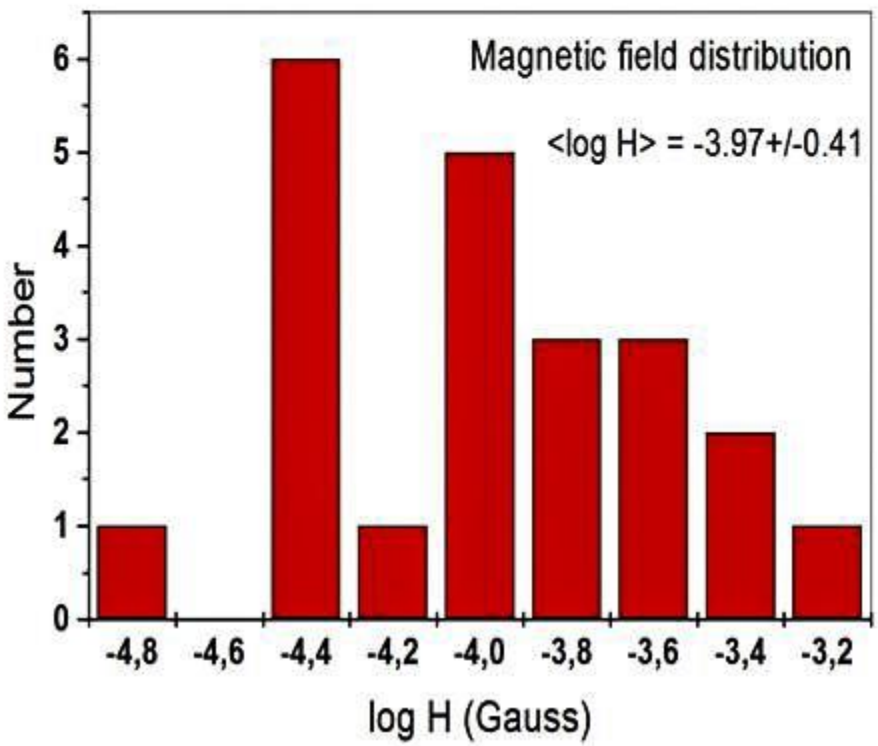

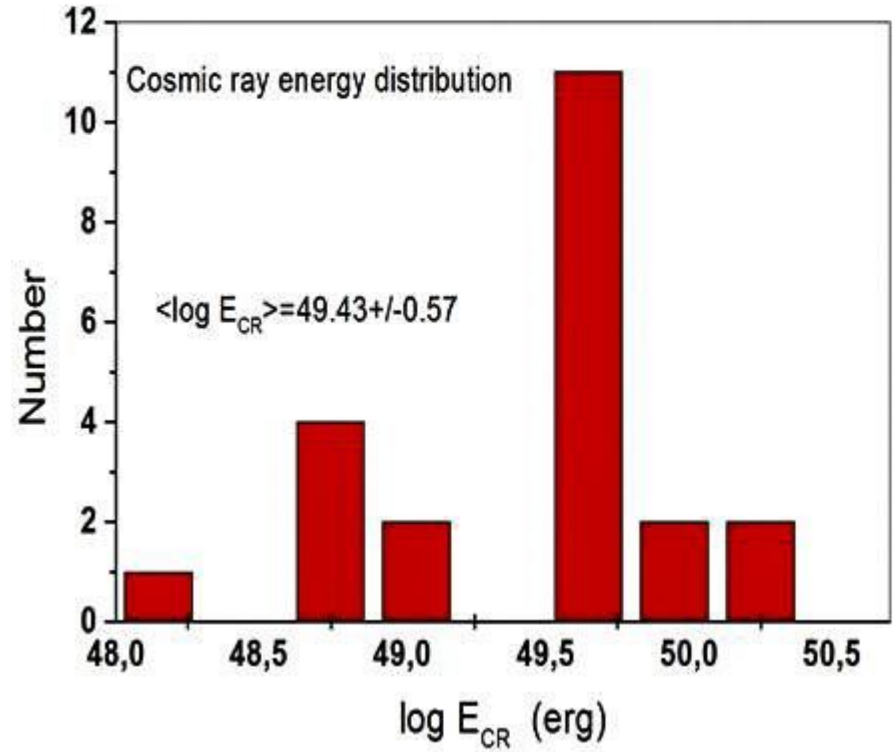

SNR from the Green catalog – Distances from the Σ_ν - R_s relation

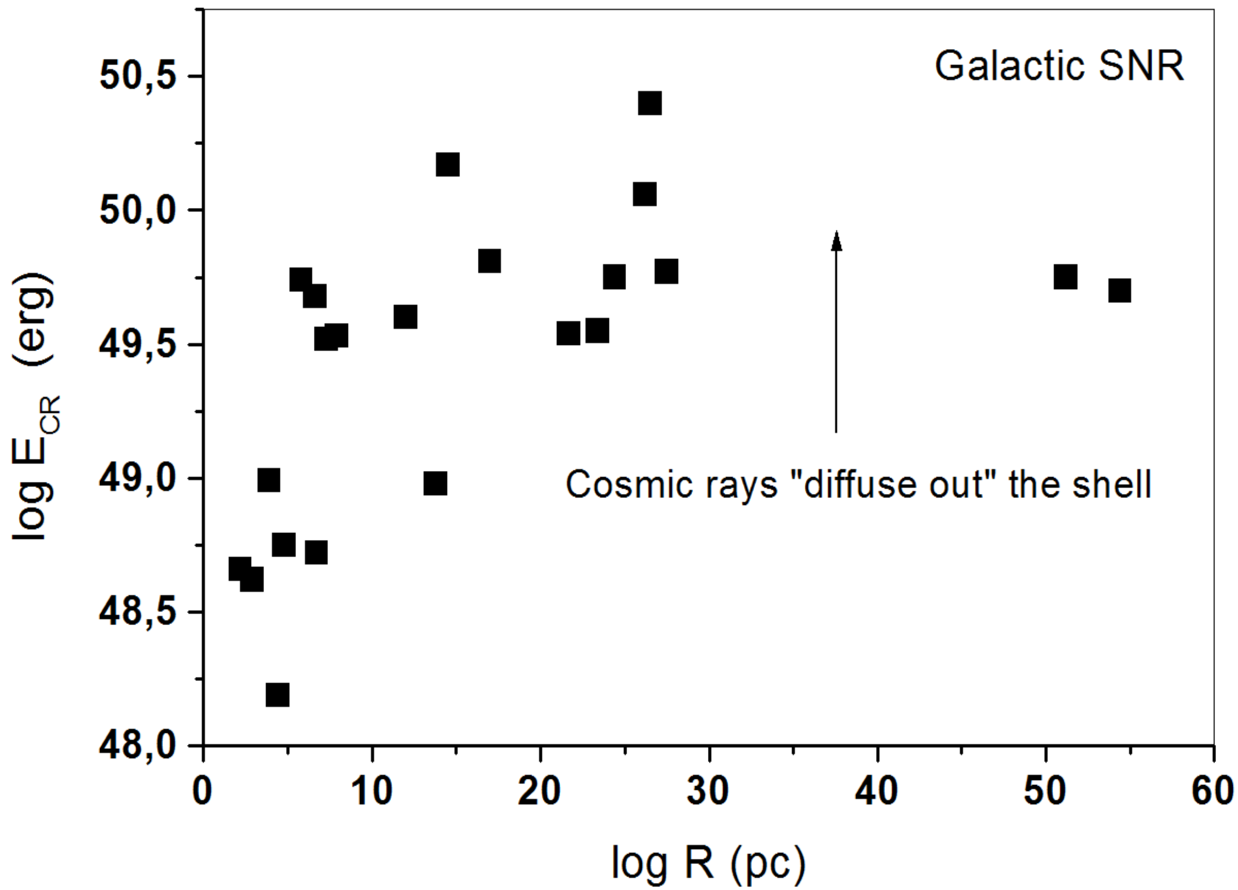

The cosmic ray energy is correlated with the shell radius up R_s ~ 40 pc. For larger radii, the relativistic particles escape to the interstellar medium

If each supernova releases about 10^{50} erg under the form of relativistic particles, then the expected cosmic ray energy density in the galactic disc is

$$w_{CR} \simeq \nu_{II} \frac{\bar{E}_{CR}}{V_d} T_{CR}$$

Since $\bar{E}_{CR} \simeq 10^{50} erg$, the volume of the disc $V_d \approx 2.4 \times 10^{66} cm^3$ and the lifetime of cosmic rays inside the confinement zone, fixed by the abundance ratio (Li+Be+B)/(C+N+O) in the cosmic ray chemical composition, is $T_{CR} \approx 1.2 \times 10^7 \, yrs$ we have

$$w_{RC} \approx 313 \nu_{II} \;\; eVcm^{-3}$$

With one SN every 240 yrs (see later) the resulting CR energy density is about 1.3 $eVcm^{-3}$, in good agreement with the observed value (1 $eVcm^{-3}$).

X-rays from the shocked region

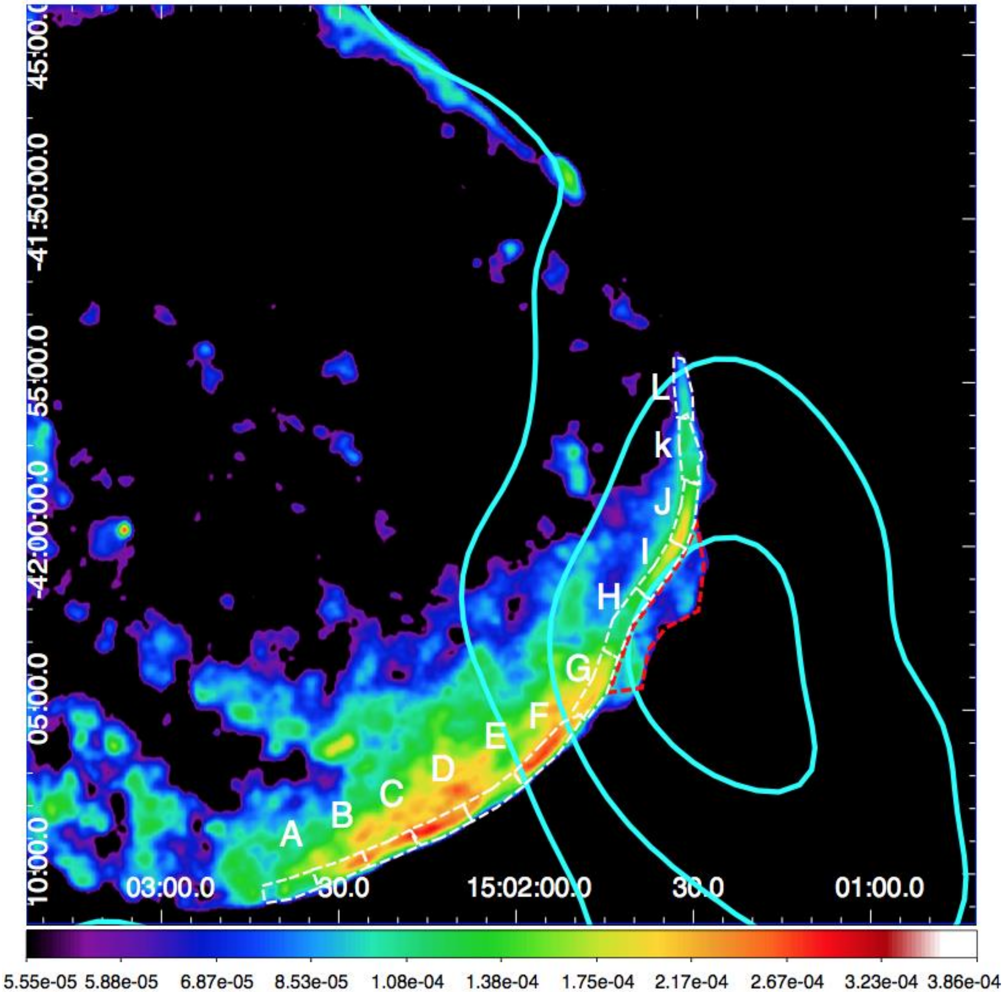

X-ray image of the SNR 1006 obtained with the satellite XMM Newton superposed to molecular CO emission.

The shock interacts with a dense molecular cloud, producing an asymmetric X-ray emission

Bremsstrahlung emission from the shocked region
Thermal X-rays

The total X-ray luminosity from the shocked region is: $L_x(\Delta\varepsilon) = \Lambda(\Delta\varepsilon, T_x) n_e n_i V_{sh}$

where: $$\Lambda(\Delta\varepsilon, T_x) = \frac{64\pi^{3/2}}{\sqrt{54}} \frac{Z^2 e^6 g}{hc^2 m} \left(\frac{kT_x}{mc^2} \right)^{1/2} \left(e^{-\varepsilon_1/kT_x} - e^{-\varepsilon_2/kT_x} \right)$$

and
$$n_e = n_p + 2n_{He} = 1.2n_p = 4.8n_0$$
$$T_s = 0.75T_x^{1.03} \quad if \quad T_x > 2keV \quad and \quad T_s = T_x \quad otherwise$$

If the distance is known, from the observed X-ray flux, the luminosity can be computed. The spectrum provides the temperature and these equations permit to derive the interstellar gas density as well as the thermal energy

$$P_s = \frac{E_{th}}{2\pi R_s^3} = n_s kT \quad \Rightarrow \quad \frac{E_{th}}{n_0} = 8\pi R_s^3 kT_s$$

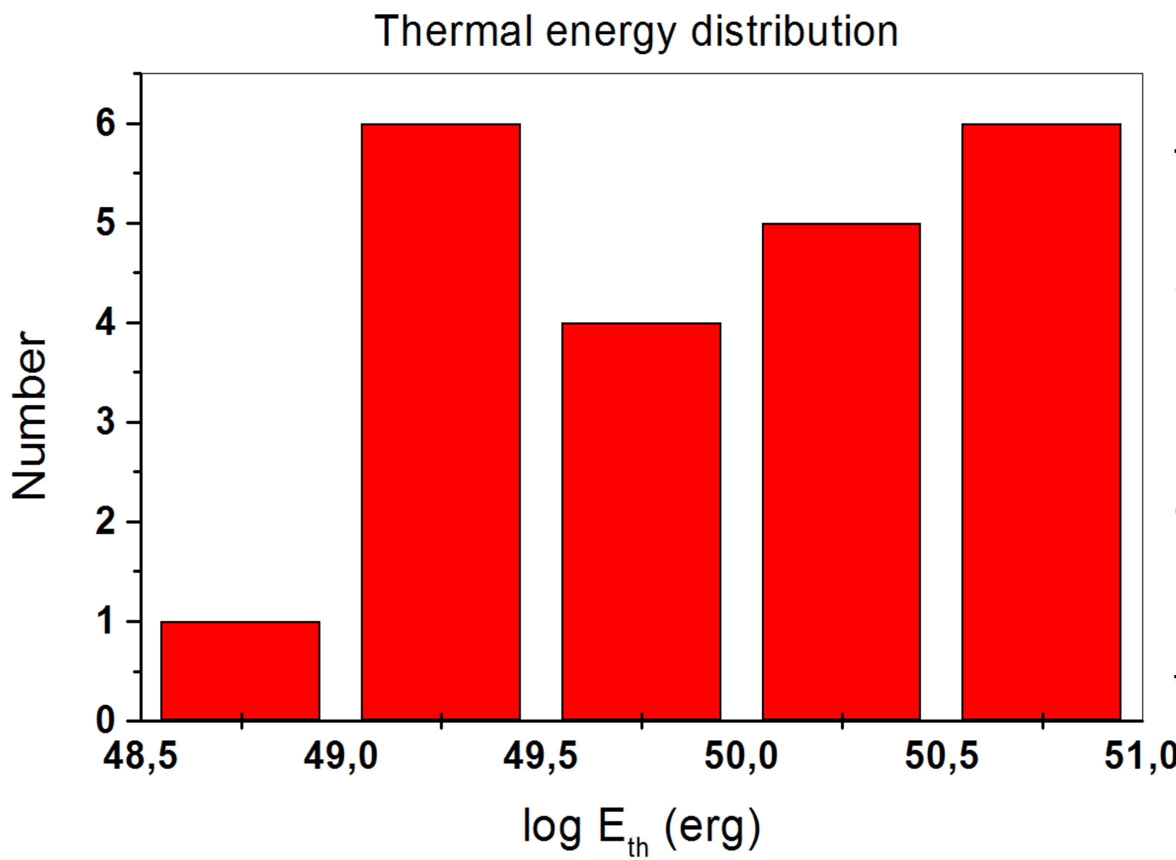

The average thermal energy inside the shocked region of SNRs is

$$\log E_{th} = 49.94 \pm 0.58$$

On the average, the energy under the form of relativistic particles represents 40% of the thermal enery

Distribution derived from data taken from the Green catalog – Distances estimated from the calibrated sigma-radius relation

Thermal energy is correlated with the shock radius

$$\log\left(\frac{E_{50}}{n_0}\right) = (-1.498 \pm 0.129) + (2.278 \pm 0.117)\log R_s \pm 0.214 \quad r^2 = 0.967$$

This relation implies for the shock velocity $\longrightarrow$ $V_s = K R_s^{-0.361}$ and for the

number of SNR less than a given radius. $N(<R_s) = 550 v_{II} R_s^{1.361}$

Comparison with data implies a frequency of about one SN each 240 yrs

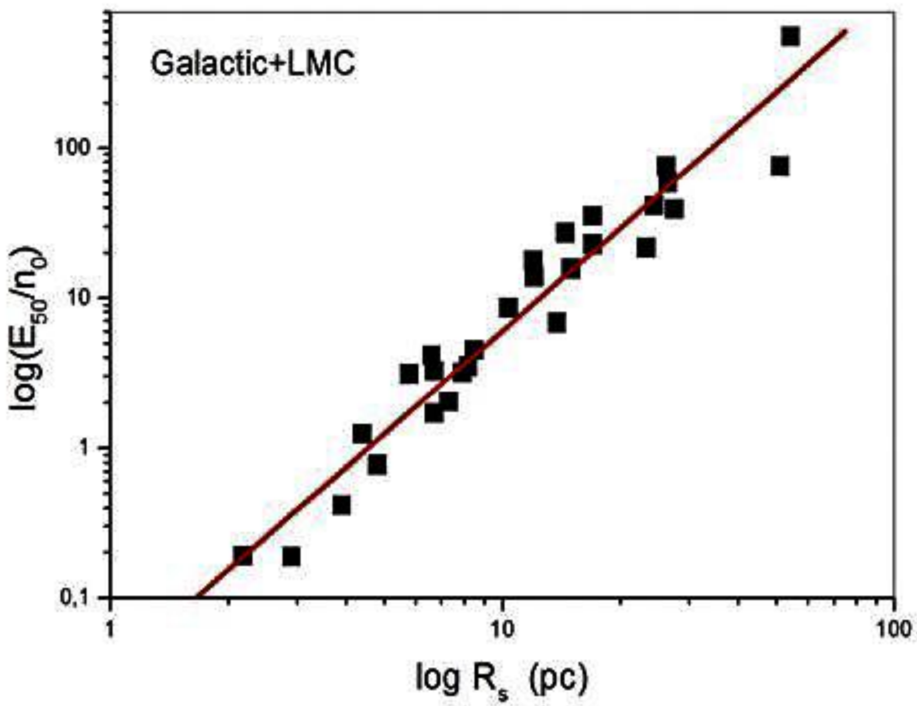

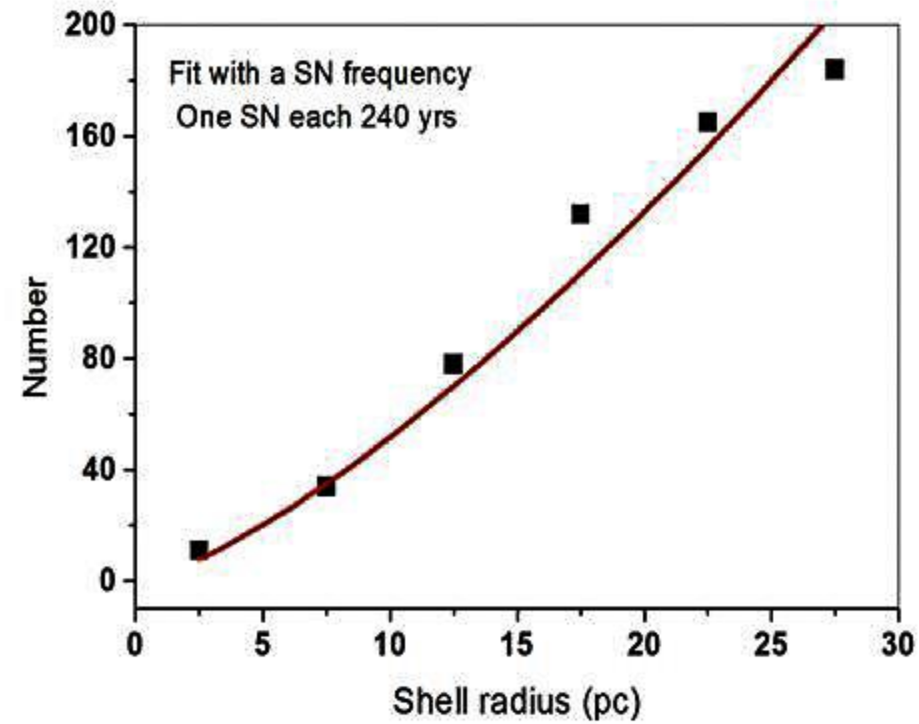

The correlation between the thermal energy & the shell radius

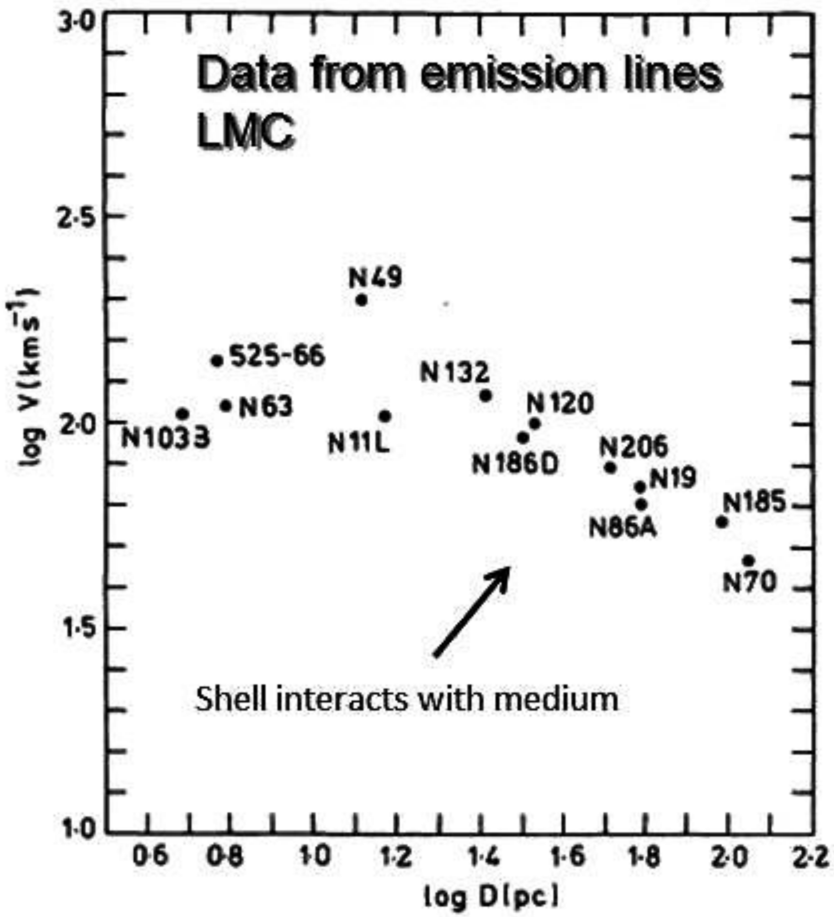

The variation of the shell velocity with radius directly from line emission data by Dopita is consistent with the results derived from X-ray data. This indicates failure in the Sedov theory.

Simulations of shock models suggest that the shell kinetic energy could be converted into thermal energy, implying that the energy content is not constant. In other words, the adiabaticity condition is not satisfied.

$$R_s > 5pc \;\; \Rightarrow \;\; V_s = 806 R_s^{-0.5} \, km/s$$

Sedov model – inhomogeneous model
(thesis – Julien Frémeaux - 2002)

Simulations of the Green catalog – goal – to simulate the same number of SNR listed in the catalog with the same brightness distribution

- Radom age from an uniform distribution (0 < t < 50 000 yrs)
- Density of a three-phase IM: dense (1 cm^{-3}); intermediate (0.1 cm^{-3}) and rarefied (0.01 cm^{-3}) - the birth probability is different for each phase
- Spectral probability according to the catalog distribution
- Explosion energy obeys a log normal distribution with a median log E = 50.0 and dispersion $\sigma_{\log} = 0.60$
- If t < $t_{crit} = 3900 n_0^{-1/3} E_{50}^{-1/2} yrs$ free expansion and if t > t_{crit} $\longrightarrow$ “Sedov”
- H-field results from the empirical $H - n_0$ relation

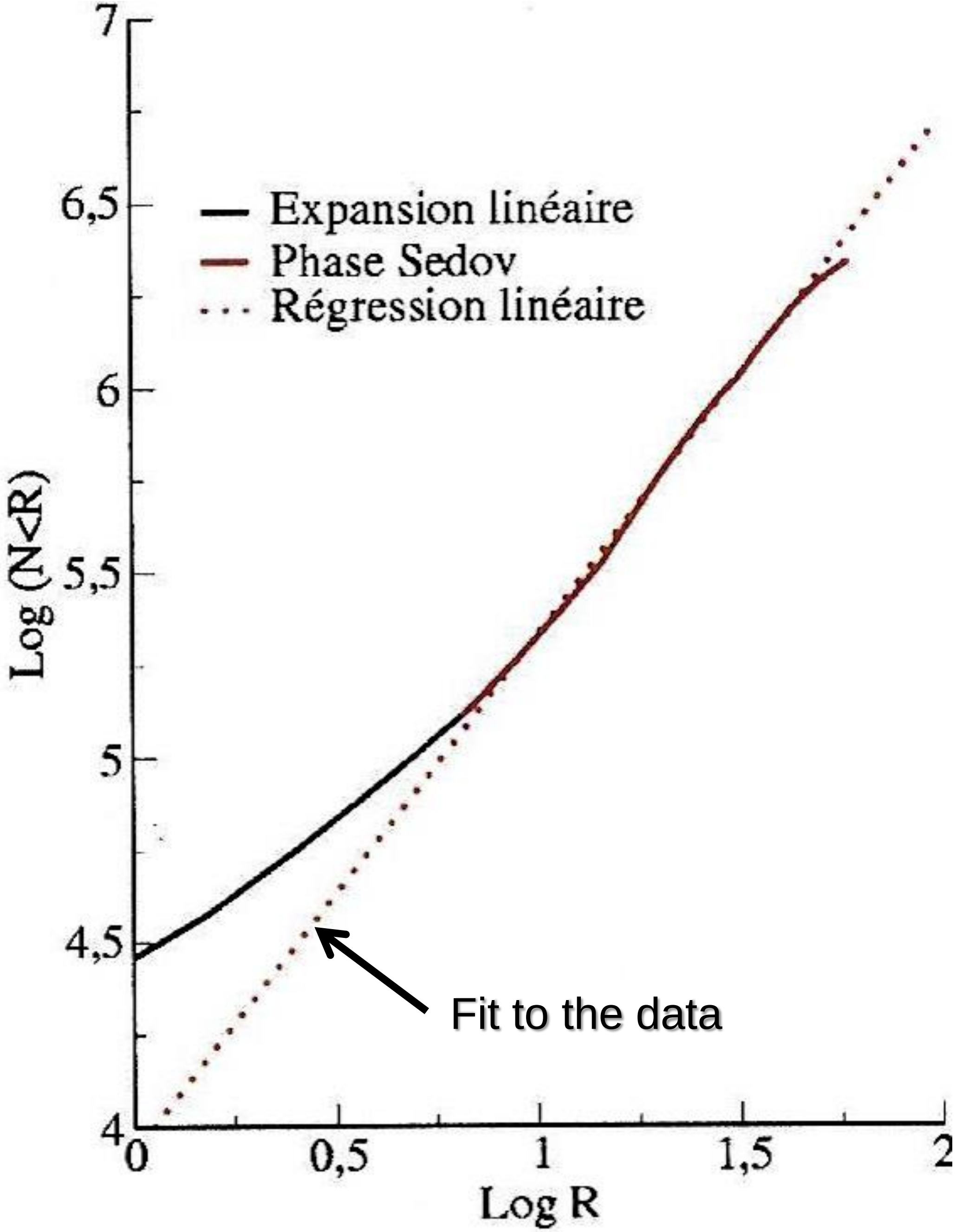

Model that provides the best fit of the brightness distribution of the catalog:

dense medium: 10%

intermediate medium: 30%

rarefied medium: 60%

$$N(<R) \propto R^{1.4}$$

An inhomogeneous medium can explain the cumulative counts even if the expansion is described by the Sedov theory!

High energy emission from SNR

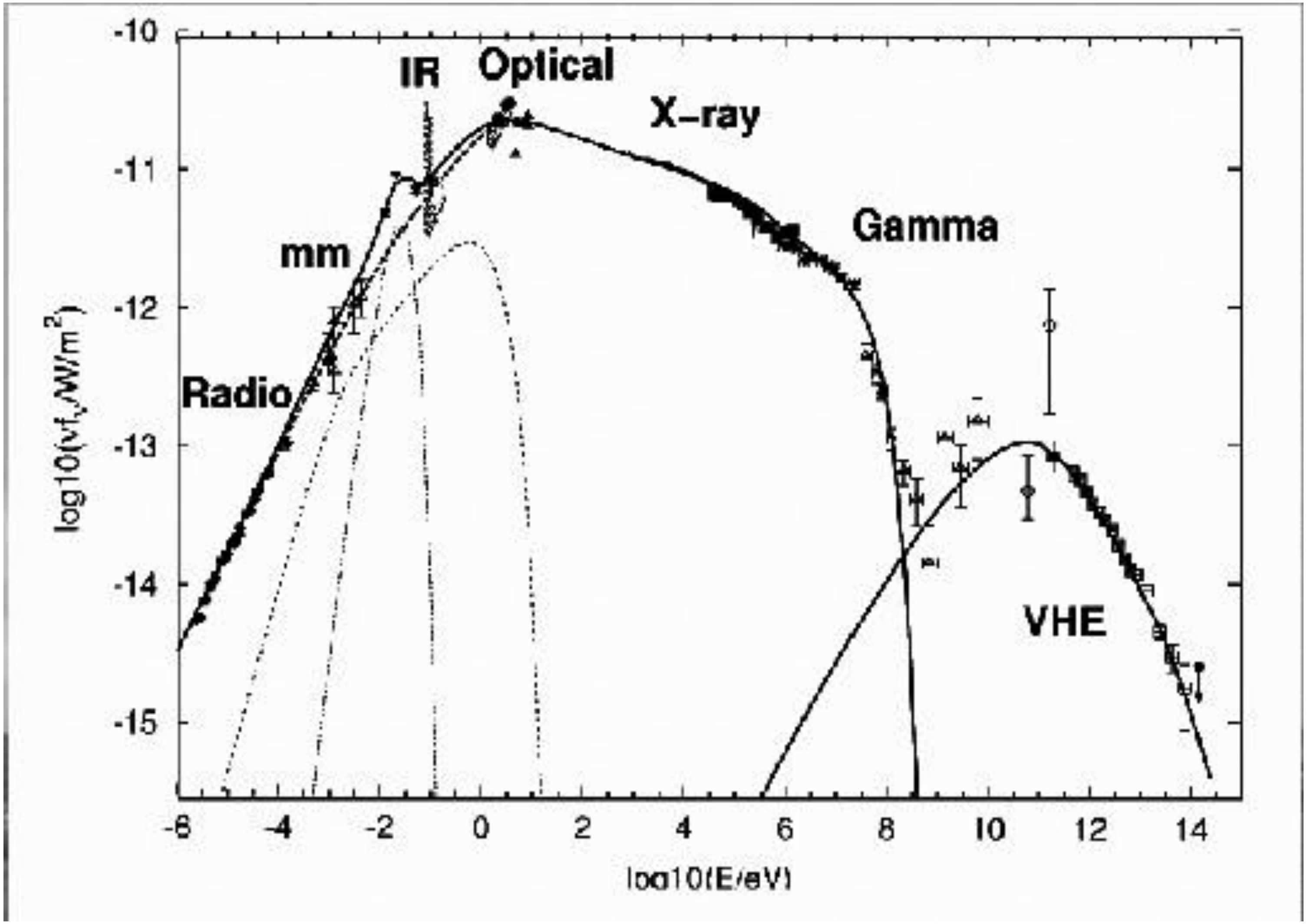

Crab remnant

Photo-pion production in SNRs

Pions are produced in SNR by CR interactions with the shell matter via

$$p + p \rightarrow p + p + a\pi^0 + b(\pi^+ + \pi^-)$$

cross section $\longrightarrow$ $\sigma_{pp}(E_p) = \sigma_0 E_p^{\beta} = 25.7 E_p^{0.08} \ mb$

multiplicity $\longrightarrow$ $\xi(E_p) = \xi_0 E_p^{\delta} \quad \delta = 0.22 \quad and \quad \xi_0 = 3.39 \quad valid \ \ for \quad E_p \geq 1 GeV$

Mean energy of pions $\longrightarrow$ $\bar{E}_\pi \approx \dfrac{E_p^{1-\delta}}{3\xi_0}$

Pion production rate: $q_\pi(E_\pi) = n_H \int N(E_p) \cdot c \cdot \xi(E_p) \sigma_{pp}(E_p) \delta(E_\pi - \bar{E}_\pi) dE_p$

where $\longrightarrow$ $N(E_p)dE_p = \dfrac{K_p}{E_p^{\gamma}} dE_p$

and $\longrightarrow$ $d\bar{E}_\pi = \dfrac{(1-\delta)}{(3\xi_0)^{1/(1-\delta)}} \bar{E}_\pi^{-\delta/(1-\delta)} dE_p$ replace this into the integral and integrate

$$q_\pi(E_\pi) = \sigma_0 n_H c K_p \frac{K_\pi}{E_\pi^{\gamma_\pi}} \quad pions/cm^3.s.GeV$$

where $\longrightarrow$
$$\begin{cases} K_\pi = \dfrac{\xi_0}{(1-\delta)(3\xi_0)^{\gamma_\pi - 1}} \quad with \quad K_{\pi^0} = \dfrac{K_\pi}{3} \quad and \quad K_{\pi^\pm} = \dfrac{2K_\pi}{3} \\ \gamma_\pi = (\gamma - \beta - 2\delta)/(1-\delta) \end{cases}$$

example: $\gamma = 2.5 \Rightarrow \gamma_\pi = 2.54 \quad K_\pi = 0.122 \quad K_{\pi^0} = 0.041 \quad K_{\pi^\pm} = 0.081$

Production of gamma-rays due to pion decay: $\pi^0 \to 2\gamma$

$$q(\varepsilon_\gamma) = 2 \int_{f(\varepsilon_\gamma)}^{\infty} q_{\pi^0}(E_{\pi^0}) \frac{dE_{\pi^0}}{\sqrt{(E_{\pi^0}^2 - 4\varepsilon_0^2)}} \quad with \quad f(\varepsilon_\gamma) = \varepsilon_\gamma + \frac{\varepsilon_0^2}{\varepsilon_\gamma} \; and \; \varepsilon_0 = 67.5\,MeV$$

Numerical solution: $q(\varepsilon_\gamma > 100MeV) = 5.28 \times 10^{-16} n_H K_p \; ph/cm^3 s$

Luminosity gamma: $L_\gamma(>100MeV) = q(>100MeV)V_s = 1.65 \times 10^{37} n_H \left(\dfrac{E_{RC}}{10^{50} erg} \right) ph/s$

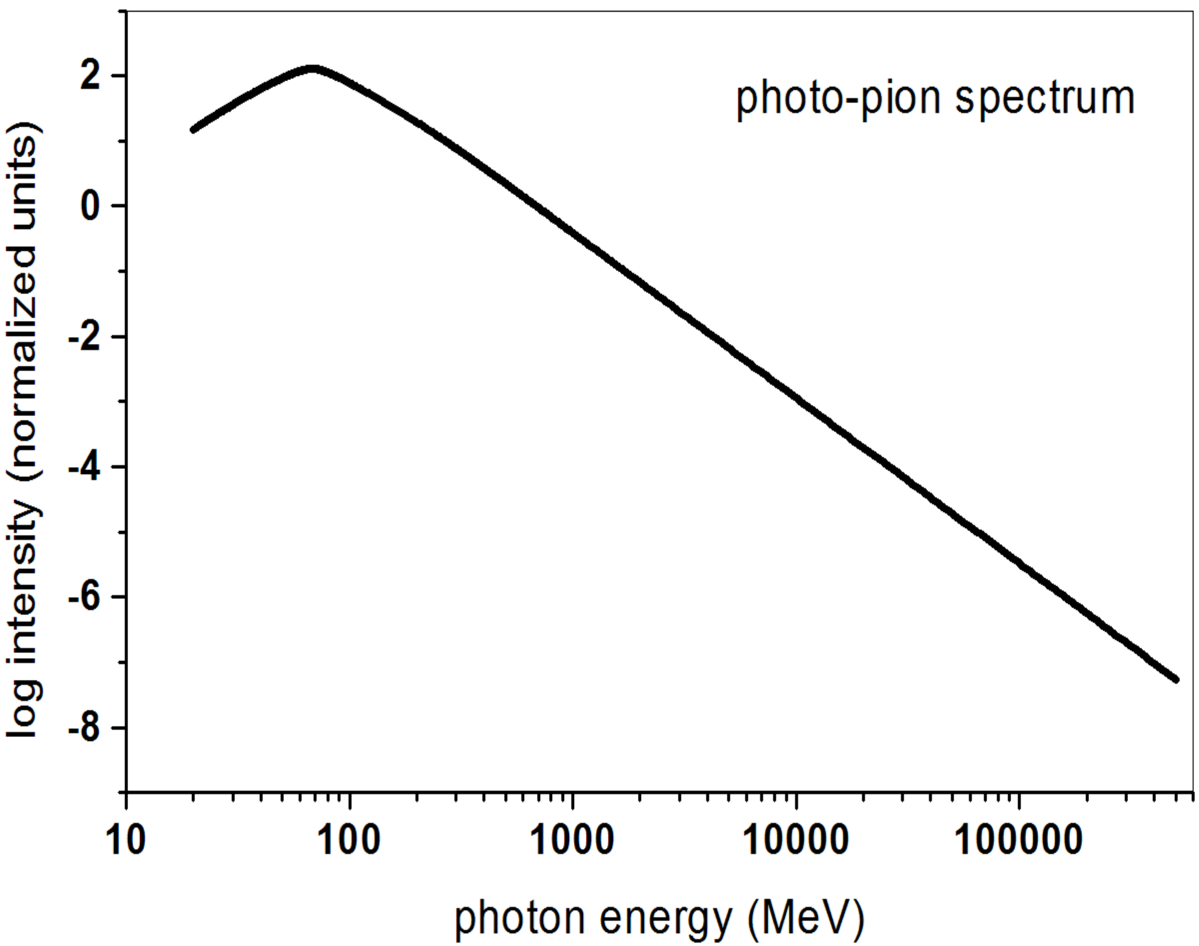

Spectrum calculated for a proton power law $\gamma_p = 2.5$

$$\varepsilon_\gamma \gg 2GeV \;\; \Rightarrow \;\; f(\varepsilon_\gamma) \propto \varepsilon_\gamma^{-2.54}$$

Muon production from pion decay $\longrightarrow$ $\pi^{\pm} \rightarrow \mu^{\pm} + \nu_{\mu}(\bar{\nu}_{\mu})$

Mean energies: $<E_{\mu}> = 0.79E_{\pi}$ $<E_{\nu_{\mu}}> = 0.21E_{\pi}$ $<E_{\nu_{\mu}}> = 0.30E_{\mu}$

Production rate of charged pions and neutrinos

$$q_{\pi^{\pm}}(E_{\pi^{\pm}}) = 6.24\times10^{-17}\frac{K_p n_H}{E_{\pi}^{\gamma_{\pi}}} \rightarrow q_{\nu_{\nu}}^{(1)} = 5.7\times10^{-18}\frac{K_p n_H}{E_{\nu_{\mu}}^{\gamma_{\pi}}}\ cm^{-3}s^{-1}GeV^{-1}$$

Neutrinos from muon decay $\longrightarrow$ $\mu^{\pm} \rightarrow e^{\pm} + \nu_{e}(\bar{\nu}_{e}) + \bar{\nu}_{\mu}(\nu_{\mu})$

Average neutrino energy: $\bar{E}_{\nu_{\mu}} = 0.3E_{\mu} \simeq 0.24E_{\pi^{\pm}}$

Neutrino production rate: $q_{\nu_{\mu}}^{(2)}(E_{\nu_{\mu}}) = 6.93\times10^{-18}\frac{K_p n_H}{E_{\nu_{\mu}}^{\gamma_{\pi}}}\ cm^{-3}s^{-1}GeV^{-1}$

Total production rate: $q_{\nu_{\mu}}^{(1)}(E_{\nu_{\mu}}) + q_{\nu_{\mu}}^{(2)} = 1.3\times10^{-17}\frac{K_p n_H}{E_{\nu_{\mu}}^{\gamma_{\pi}}}\ cm^{-3}s^{-1}GeV^{-1}$

Expected muon-neutrino flux: $f_{\nu} = \frac{q_{\nu}V_{sh}}{4\pi D^{2}}$

Some examples

Supernova	γ	Log E_{CR} (erg)	D (kpc)	n_0 (cm^{-3})
Kepler	2.28	48.66	5.0	0.84
G119.5+10.2	2.20	49.77	2.1	0.0041
G132.7+1.3	2.20	49.75	2.1	0.027
G315.4-2.3	2.20	48.72	1.1	0.099
G327.6+14.6	2.20	48.19	1.0	0.23
G53.6-2.2	2.50	50.40	6.0	0.085

Supernova	f_γ(>100 MeV) $cm^{-2}s^{-1}$	f_γ(>1.0 TeV) $cm^{-2}s^{-1}$	f_γ(>10 GeV) $cm^{-2}s^{-1}$
Kepler	**3.0×10^{-10}**	**3.0×10^{-15}**	**8.1×10^{-13}**
G119.5+10.2	**7.6×10^{-11}**	**1.5×10^{-15}**	**2.9×10^{-13}**
G132.7+1.3	**4.7×10^{-10}**	**9.7×10^{-15}**	**1.8×10^{-12}**
G315.4-2.3	**5.2×10^{-10}**	**1.3×10^{-14}**	**2.2×10^{-12}**
G327.6+14.6	**4.3×10^{-10}**	**1.1×10^{-14}**	**1.9×10^{-12}**
G53.6-2.2	**3.2×10^{-9}**	**2.4×10^{-15}**	**2.4×10^{-12}**

SN 1987A – LMC – already 30 years!

- February 1987
- 22.4 UT : the progenitor – Sand -69°.202 (B2I) detected at V =12.2
- 23.12 UT : 5 neutrino pulses ($E\nu$ > 7 MeV) detected by Mont Blanc detector
- 23.316 UT : 11 neutrino events ($7.5 < E\nu < 36$ MeV) detected by Kamiokande II (Mont Blanc neutrinos were not seen)
- 23.316 UT : 8 neutrino events with $E\nu < 50$ MeV detected at Irvine-Michigan-Brookhaven experiment
- 23.316 UT : 3 neutrino events seen at Baksan with $E\nu \sim 20$ MeV
- 24.23 UT : discovery by I. Shelton the “optical” SN at V ~ 5.1
- 26.8 UT: beginning of the observations at LNA

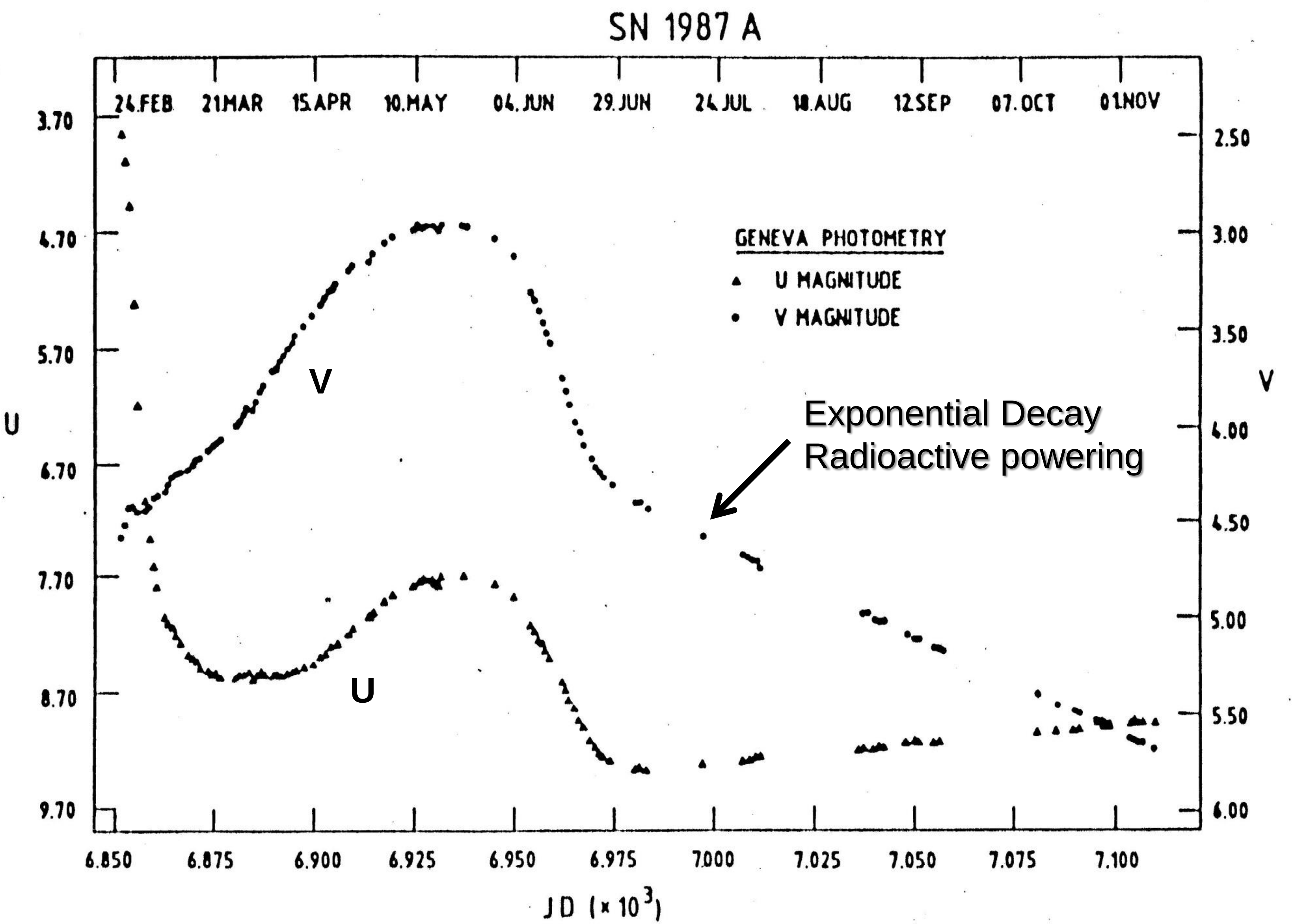

SN 1987 A
26.FEB
21.MAR
15.APR
10.MAY
04.JUN
29.JUN
24.JUL
18.AUG
12.SEP
07.OCT
01.NOV
GENEVA PHOTOMETRY
U MAGNITUDE
V MAGNITUDE
Exponential Decay
Radioactive powering
V
U
3.70
4.70
5.70
6.70
7.70
8.70
9.70
2.50
3.00
3.50
4.00
4.50
5.00
5.50
6.00
6.850
6.875
6.900
6.925
6.950
6.975
7.000
7.025
7.050
7.075
7.100
JD (× 10^3)

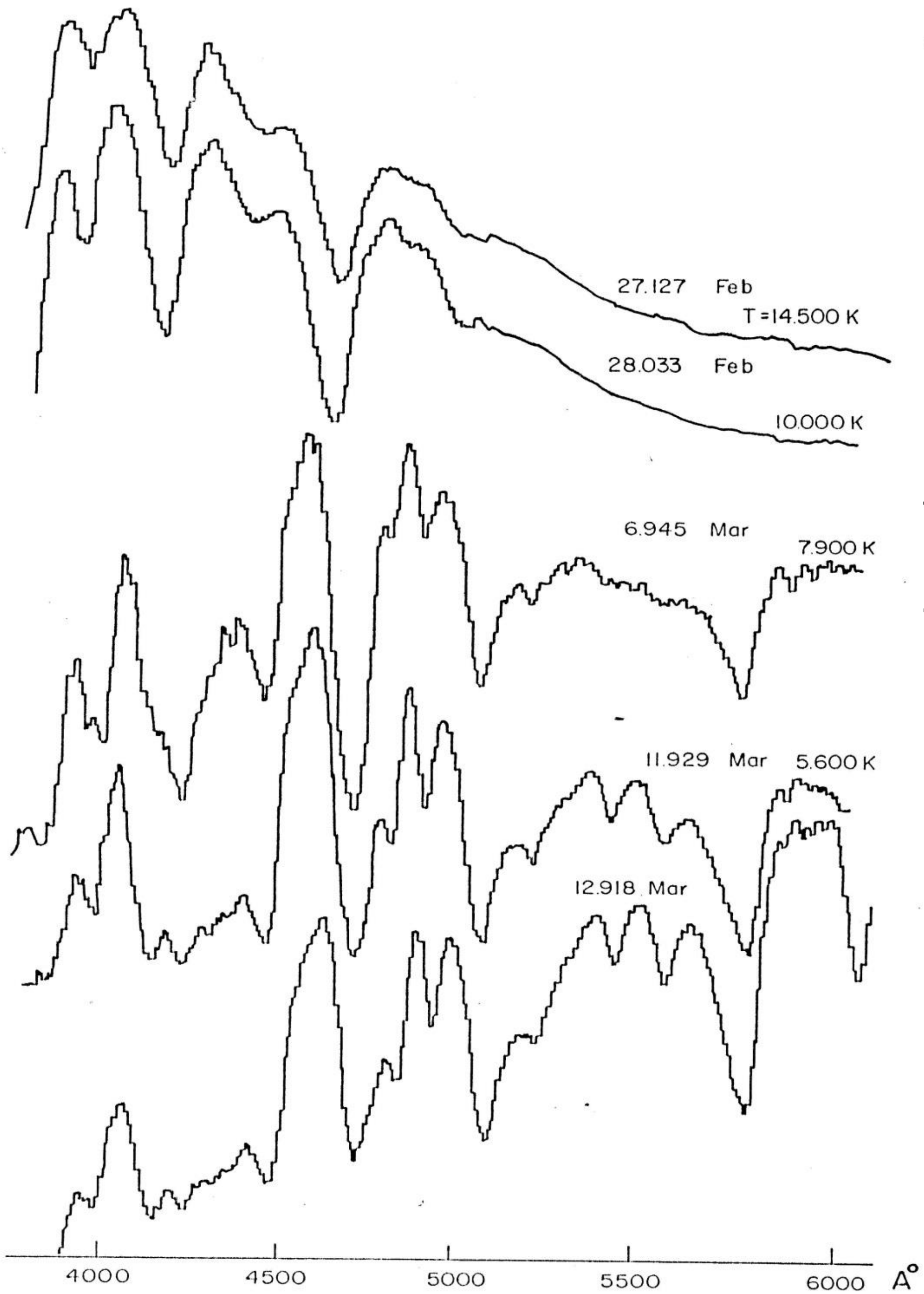

First spectra obtained at LNA – these spectra are dominated by broad absorption bands. The envelope was still opaque.

Fit of the continuum permitted an estimation of the color temperature of the expanding atmosphere.

The radius of the expanding atmosphere was estimated from

$$f_\lambda = \left(\frac{R_*}{D}\right)^2 \pi B_\lambda(T_c)$$

First results – MNRAS 240, 179, 1989

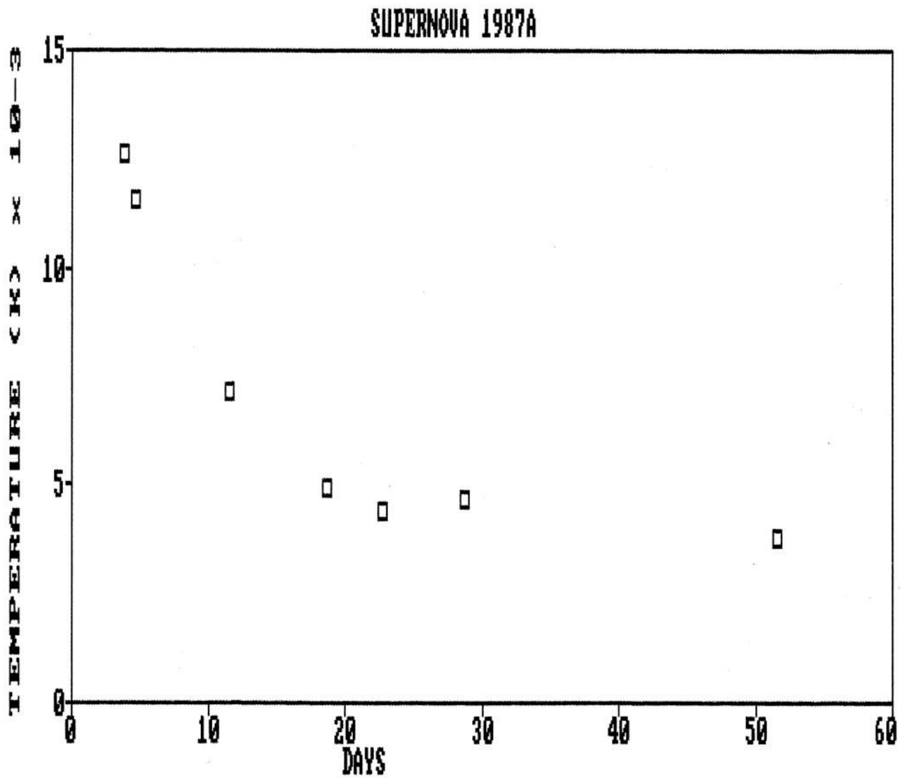

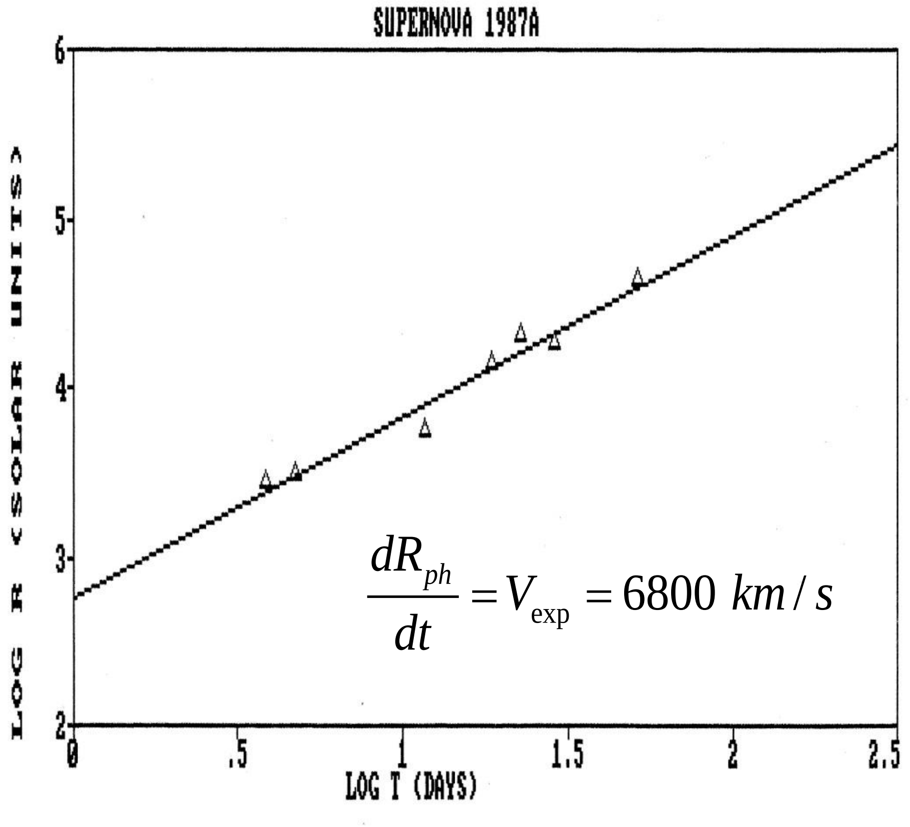

Color temperature – derived from black body fits of the continuum

Evolution of the apparent photospheric radius calculated as explained before – the time derivative gives the expansion velocity of the photosphere

Line Identification: Spectrum Taken on March 12.92 UT, 1987

λ_{obs} (Å)	Identification	E_ℓ (eV)	W_λ (Å)
4737	Hβλ4861	10.2	92.2
	FeIλ4872	2.89	
4842	FeIλ4920	2.84	43.5
	FeIIλ4923	2.88	
	BaIIλ4934	0.00	
4940	FeIλ5012	3.93	28.2
	FeIIλ5018	2.88	
5100	FeIIλ5169	2.88	111.4
	MgIλ5183	2.71	
5240	FeIλ5324	3.21	62.6
	FeIIλ5316,62	2.84	
	CaIλ5349	2.68	
5452	CaIλ5588	2.50	23.4
	ScIIλ5526	1.77	
	MgIλ5528	4.35	
5570	ScIIλ5658	1.50	40.0
	FeIλ5615,24,58	3.33	
5800	NaIλ5890	0.00	103.3
	BaIIλ5854	0.60	
	CaIλ5857,67	2.91	
6052	CaIλ6162	1.86	26.7
	CaIλ6169	2.50	
	BaIIλ6142	0.70	

Proposed identification of the observed absorption features: a difficult task caused by the blending of the broad lines.

Line profiles modeled by the Sobolev theory

Derived abundances

$$\frac{Na}{Fe} = 0.1\ (0.045)_\odot \qquad \frac{Mg}{Fe} = 0.55\ (0.66)_\odot$$

$$\frac{Sc}{Fe} = 4.6\times10^{-4}\ \ (4.1\times10^{-5})_\odot$$

$$\frac{Ba}{Fe} = 3.5\times10^{-6}\ \ (2.2\times10^{-6})_\odot$$

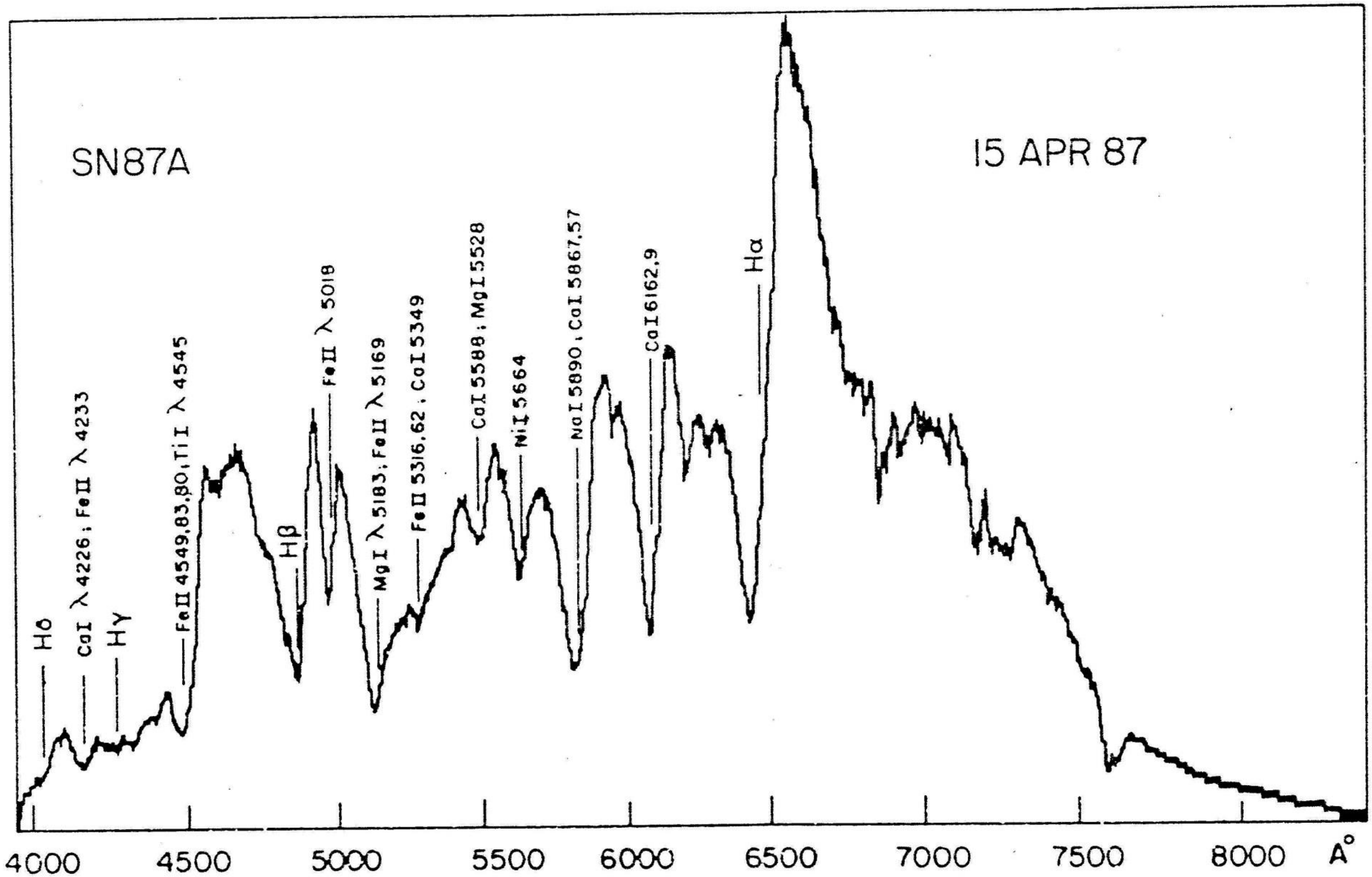

Emission features begin to appear

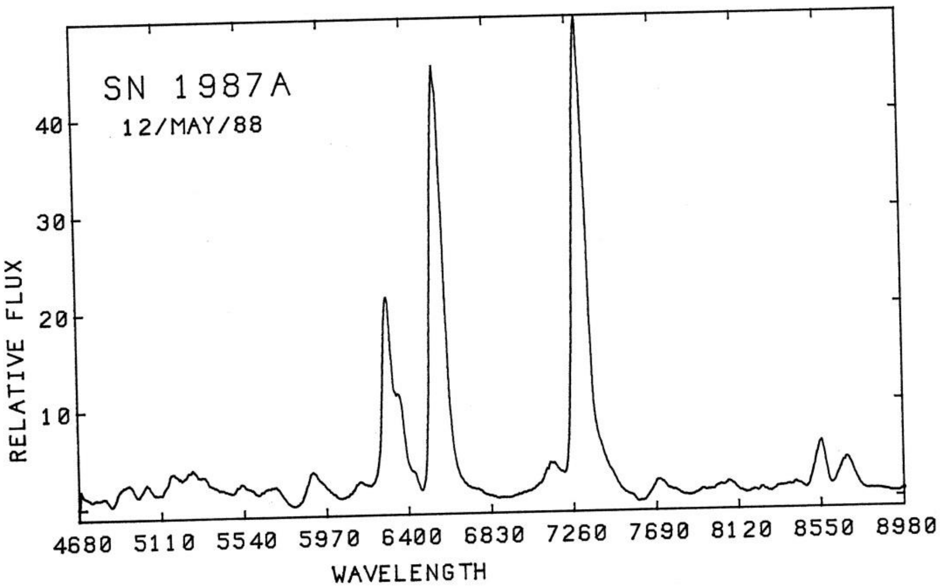
SN 1987A
12/MAY/88
RELATIVE FLUX
10
20
30
40
4680
5110
5540
5970
6400
6830
7260
7690
8120
8550
8980
WAVELENGTH

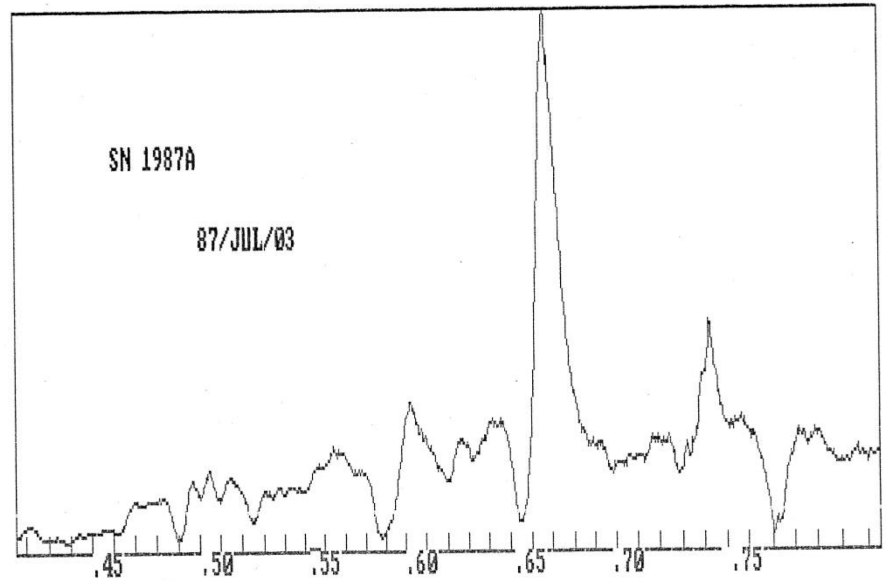
SN 1987A
87/JUL/03
.45
.50
.55
.60
.65
.70
.75

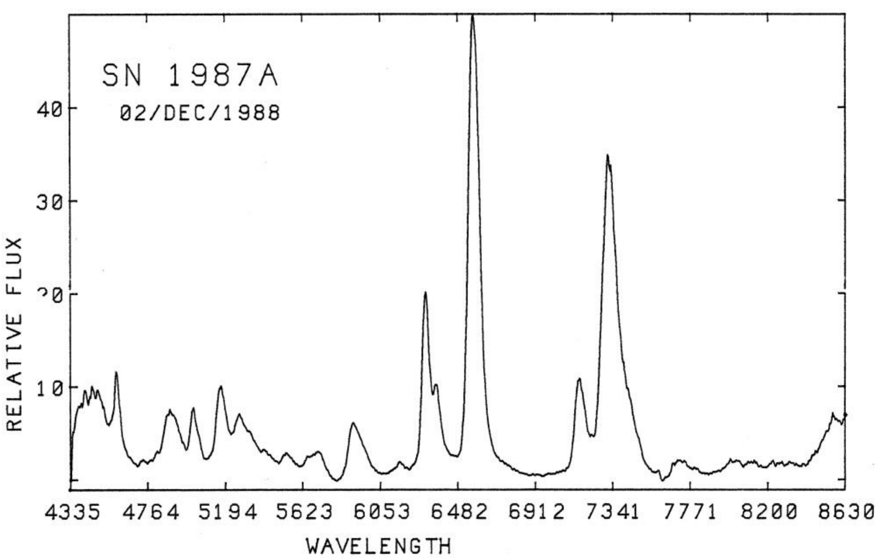
SN 1987A
02/DEC/1988
RELATIVE FLUX
10
20
30
40
4335
4764
5194
5623
6053
6482
6912
7341
7771
8200
8630
WAVELENGTH

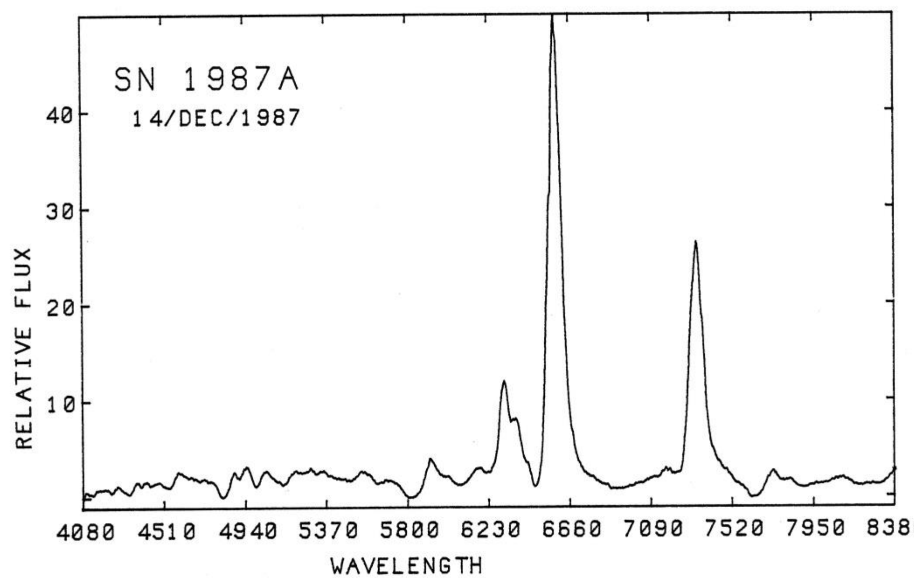
SN 1987A
14/DEC/1987
RELATIVE FLUX
10
20
30
40
4080
4510
4940
5370
5800
6230
6660
7090
7520
7950
8380
WAVELENGTH

LINE FLUXES

(in units of 10^{-11} erg.cm^{-2}s^{-1})

Ion	Day 294	Day 646
H λ4101	-	1.4
FeIIλ4233 } CaIλ4266 }	-	1.4
CaIλ4302	-	2.7
[FeII]λ4359	9.8	3.5
[FeII]λ4416	13.2	3.8
[FeII]λ4475	14.4	3.5
MgI]λ4571	25.7	1.7
[FeII]λ4728	11.4	1.6
Hβλ4861	15.8	2.0
FeIIλ4923	41.8	1.0
FeIIλ5018	28.3	1.7
FeIIλ5169	-	3.5
[FeII]λ5527	9.3	1.6
[OI]λ5577	26.3	0.14
NaIλ5890,95	80.9	2.7
NaIλ6154? } CaIλ6162? }	90.3	0.30
[OI]λ6300,63	388.2	8.6
Hαλ6563	1487	22.3
[FeII]λ7155	78.2	5.5
[CaII]λ7316	780.4	22.6

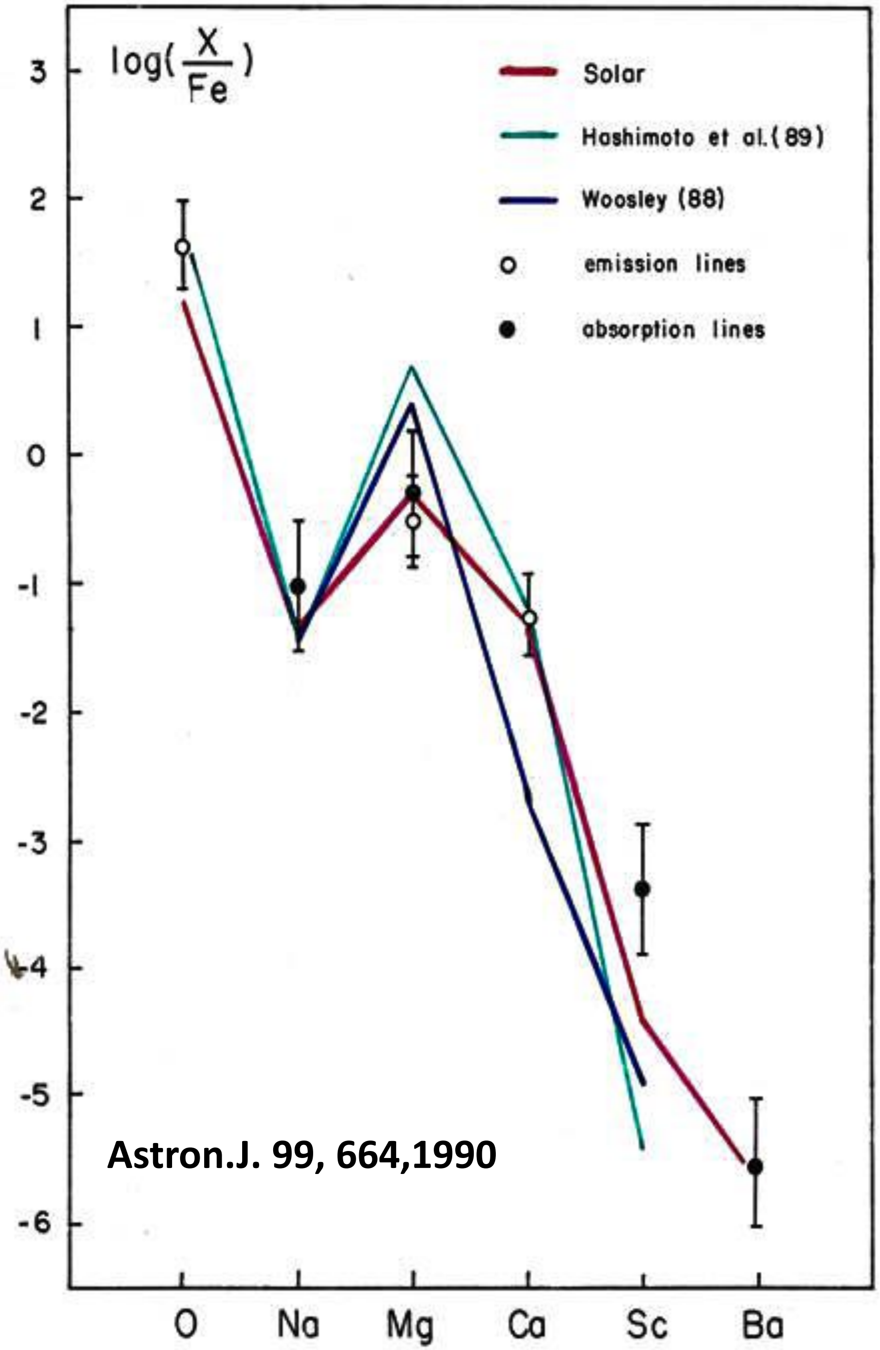

What SN1987A has taught us

- The detection of neutrino pulses confirms the gravitational collapse scenario in which a neutron core is formed

- However, no pulsar was detected up to now. This means that whether the beam does not sweep the Earth or a fraction of the envelope has fallen back leading to a BH formation

- The late evolution of the light curve is due to the radioactive decay of ^{56}Co – Nuclear lines of cobalt (0.847 and 1.238 MeV) were detected confirming powering of the envelope by radioactivity. A cobalt mass of 0.07 $M_\odot$ was present in the ejecta.

- Ejected oxygen and iron masses are in agreement with the “onion model” envelope